

BRL R 1541

AD

BRL

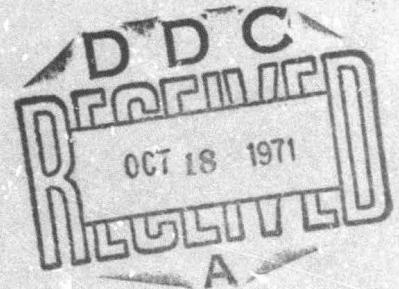
REPORT NO. 1541

A NUMERICAL SOLUTION FOR FLOW BETWEEN ROTATING AND STATIONARY FINITE DISKS

by

Donald H. McCoy

June 1971



This document has been approved for public release and sale;
its distribution is unlimited.

Reproduced by
NATIONAL TECHNICAL
INFORMATION SERVICE
Springfield, Va. 22151

U.S. ARMY ABERDEEN RESEARCH AND DEVELOPMENT CENTER
BALLISTIC RESEARCH LABORATORIES
ABERDEEN PROVING GROUND, MARYLAND

AD 731 217

52

Destroy this report when it is no longer needed.
Do not return it to the originator.

Secondary distribution of this report by originating or
sponsoring activity is prohibited.

Additional copies of this report may be purchased from the
U.S. Department of Commerce, National Technical Information
Service, Springfield, Virginia 22151.

ACCESSION for

CFSTI WHITE SECTION
DDC BUFF SECTION

UNANNOUNCED
JUSTIFICATION

BY

DISTRIBUTION/AVAILABILITY CODES

DIST.	AVAIL.	AND/OR	SPECIAL
A			

The findings in this report are not to be construed as
an official Department of the Army position, unless
so designated by other authorized documents.

Unclassified

Security Classification

DOCUMENT CONTROL DATA - R & D

(Security classification of title, body of abstract and indexing annotation must be entered when the overall report is classified)

1. ORIGINATING ACTIVITY (Corporate author) US Army Aberdeen Research and Development Center Ballistic Research Laboratories Aberdeen Proving Ground, Maryland 21005	2a. REPORT SECURITY CLASSIFICATION Unclassified
2b. GROUP	

3. REPORT TITLE
A NUMERICAL SOLUTION FOR FLOW BETWEEN ROTATING AND STATIONARY FINITE DISKS

4. DESCRIPTIVE NOTES (Type of report and inclusive dates)

5. AUTHOR(S) (First name, middle initial, last name)
Donald H. McCoy

6. REPORT DATE June 1971	7a. TOTAL NO. OF PAGES 55	7b. NO. OF REFS 4
-----------------------------	------------------------------	----------------------

8a. CONTRACT OR GRANT NO. A. PROJECT NO. RDT&E 1T562603A041	8b. ORIGINATOR'S REPORT NUMBER(S) BRL Report No. 1541
8c.	8d. OTHER REPORT NO(S) (Any other numbers that may be assigned this report)

10. DISTRIBUTION STATEMENT
This document has been approved for public release and sale; its distribution is unlimited.

11. SUPPLEMENTARY NOTES	12. SPONSORING MILITARY ACTIVITY US Army Materiel Command Washington, D. C.
-------------------------	---

13. ABSTRACT
The velocity field and pressure distribution between stationary and rotating finite disks are obtained by a finite difference solution of the Navier-Stokes equations and the continuity equation using an explicit scheme developed by Chorin [1]. These numerical results are compared with the results of "infinite disk" solutions. In the range of interest for viscometer applications, the velocity and pressure are adequately represented by the infinite disk solutions.

14. KEY WORDS	LINK A		LINK B		LINK C	
	ROLE	WT	ROLE	WT	ROLE	WT
Navier-Stokes Equations Fluid Flow Viscometer						

BALLISTIC RESEARCH LABORATORIES

REPORT NO. 1541

JUNE 1971

**A NUMERICAL SOLUTION FOR
FLOW BETWEEN ROTATING AND
STATIONARY FINITE DISKS**

Donald H. McCoy

Exterior Ballistics Laboratory

**This document has been approved for public release and sale;
its distribution is unlimited.**

RDT&E Project No. 1T562603A041

ABERDEEN PROVING GROUND, MARYLAND

BALLISTIC RESEARCH LABORATORIES

REPORT NO. 1541

DHMcCoy/ajb
Aberdeen Proving Ground, Md.
June 1971

A NUMERICAL SOLUTION FOR
FLOW BETWEEN ROTATING AND
STATIONARY FINITE DISKS

ABSTRACT

The velocity field and pressure distribution between stationary and rotating finite disks are obtained by a finite difference solution of the Navier-Stokes equations and the continuity equation using an explicit scheme developed by Chorin [1]. These numerical results are compared with the results of "infinite disk" solutions. In the range of interest for viscometer applications, the velocity and pressure are adequately represented by the infinite disk solutions.

TABLE OF CONTENTS

	Page
ABSTRACT	3
TABLE OF SYMBOLS	7
I. INTRODUCTION	9
II. THE EQUATIONS OF MOTION	10
III. NUMERICAL PROCEDURE	13
IV. STABILITY	21
V. NUMERICAL RESULTS AND DISCUSSION	22
VI. CONCLUSIONS	29
VII. REFERENCES	33
APPENDIX A	34
APPENDIX B	41
DISTRIBUTION LIST	53

TABLE OF SYMBOLS

Symbol	Definition
D	Artificial density
N	Number of iterations
p	Pressure
P	Dimensionless pressure, D/δ
(r, θ , z)	Cylindrical coordinates
(R, θ , Z)	Dimensionless cylindrical coordinates
\bar{R}	Maximum radial distance
R_e	Reynolds number
t	Time
T	Dimensionless time
u	Radial velocity
U	Dimensionless radial velocity
U_∞	Dimensionless radial velocity from the infinite disk solution

v	Tangential velocity	
V	Dimensionless tangential velocity	
w	Axial velocity	
W	Dimensionless axial velocity	
\bar{z}	Maximum axial distance	
δ	Artificial compressibility factor	
λ	Ratio, \bar{z}/\bar{R}	
μ	Viscosity	
ν	Kinematic viscosity, μ/ρ	
ρ	Density	
Ω	Angular velocity	
		Reynolds number
		Time
		Dimensionless time
		Radial velocity
		Dimensionless radial velocity
		Dimensionless radial velocity from the infinite disk solution

I. INTRODUCTION

The problem of practical interest to be solved can be stated as follows: An incompressible Newtonian liquid is contained between an upper, stationary disk and a lower, rotating disk. Determine the velocity field and pressure distribution of the fluid in motion.

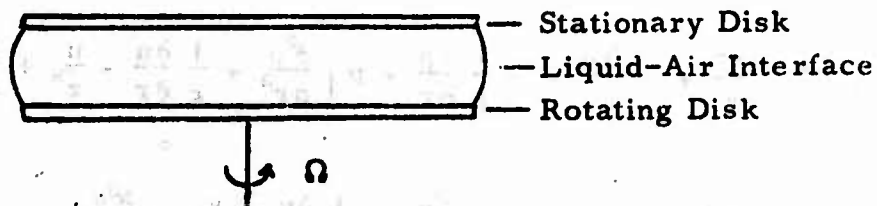


Figure 1. Physical Configuration

By presenting accurate numerical solutions to the Navier-Stokes equations, this paper makes possible an effective determination of the nature of inertial secondary motions in a rotating disk viscometer having disks of finite radii. Previous considerations of the problem have assumed that the disks are of infinite radii, resulting in solutions involving numerical and analytical approximations [2, 3]. A comparison will be made of the velocity distributions obtained with disks of finite radii and those having radii assumed to be infinite.

II. THE EQUATIONS OF MOTION

The equations governing flow consist of those of Navier-Stokes together with the equation for continuity. These, as used in this paper, are for a cylindrical coordinate system (r, θ, z) with rotational symmetry and incompressibility assumed. The equations are written as follows [4]:

$$\frac{\partial u}{\partial t} + u \frac{\partial u}{\partial r} - \frac{v^2}{r} + w \frac{\partial u}{\partial z} = -\frac{1}{\rho} \frac{\partial p}{\partial r} + \nu \left[\frac{\partial^2 u}{\partial r^2} + \frac{1}{r} \frac{\partial u}{\partial r} - \frac{u}{r^2} + \frac{\partial^2 u}{\partial z^2} \right] \quad (1)$$

$$\frac{\partial v}{\partial t} + u \frac{\partial v}{\partial r} + \frac{uv}{r} + w \frac{\partial v}{\partial z} = \nu \left[\frac{\partial^2 v}{\partial r^2} + \frac{1}{r} \frac{\partial v}{\partial r} - \frac{v}{r^2} + \frac{\partial^2 v}{\partial z^2} \right] \quad (2)$$

$$\frac{\partial w}{\partial t} + u \frac{\partial w}{\partial r} + w \frac{\partial w}{\partial z} = -\frac{1}{\rho} \frac{\partial p}{\partial z} + \nu \left[\frac{\partial^2 w}{\partial r^2} + \frac{1}{r} \frac{\partial w}{\partial r} + \frac{\partial^2 w}{\partial z^2} \right] \quad (3)$$

$$\frac{u}{r} + \frac{\partial u}{\partial r} + \frac{\partial w}{\partial z} = 0 \quad (4)$$

Here, u , v , and w represent, respectively, velocities in the radial, tangential, and axial directions. ρ is density; p is pressure; and ν is kinematic viscosity. The radius of each disk is R ; the spacing between them is \bar{Z} ; and the angular velocity of the rotating disk is Ω .

The above equations are normalized according to the following procedure:

Primary Variable	Normalizing Quantity	Normalized Variable
u, v, w	$\bar{R}\Omega$	U, V, W
r	\bar{R}	R
z	\bar{Z}	Z
t	$\bar{Z}/\bar{R}\Omega$	T
p	$\rho \bar{R}^2 \Omega^2$	P

The normalized equations are

$$\frac{\partial U}{\partial T} + \lambda \left(U \frac{\partial U}{\partial R} - \frac{V^2}{R} \right) + W \frac{\partial U}{\partial Z} = -\lambda \frac{\partial P}{\partial R} + \frac{1}{R_e} \left[\lambda^2 \left(\frac{\partial^2 U}{\partial R^2} + \frac{1}{R} \frac{\partial U}{\partial R} - \frac{U}{R^2} \right) + \frac{\partial^2 U}{\partial Z^2} \right] \quad (5)$$

$$\frac{\partial V}{\partial T} + \lambda \left(U \frac{\partial V}{\partial R} + \frac{UV}{R} \right) + W \frac{\partial V}{\partial Z} = \frac{1}{R_e} \left[\lambda^2 \left(\frac{\partial^2 V}{\partial R^2} + \frac{1}{R} \frac{\partial V}{\partial R} - \frac{V}{R^2} \right) + \frac{\partial^2 V}{\partial Z^2} \right] \quad (6)$$

$$\frac{\partial W}{\partial T} + \lambda U \frac{\partial W}{\partial R} + W \frac{\partial W}{\partial Z} = -\frac{\partial P}{\partial Z} + \frac{1}{R_e} \left[\lambda^2 \left(\frac{\partial^2 W}{\partial R^2} + \frac{1}{R} \frac{\partial W}{\partial R} \right) + \frac{\partial^2 W}{\partial Z^2} \right] \quad (7)$$

$$\lambda \left(\frac{U}{R} + \frac{\partial U}{\partial R} \right) + \frac{\partial W}{\partial Z} = 0 \quad (8)$$

where $R_e = \frac{\bar{Z}\bar{R}\Omega}{\nu}$ and $\lambda = \bar{Z}/\bar{R}$.

The boundary conditions used are shown in Figure 2.

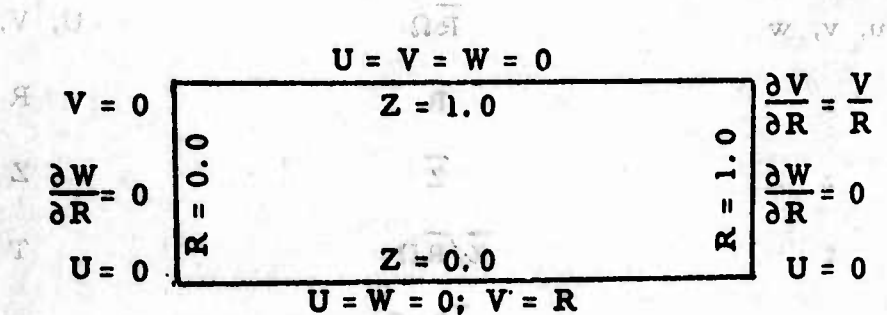


Figure 2. Boundary Conditions

The rotating plate is at $Z = 0$ and the stationary one at $Z = 1$. $R = 0$ is the axis of rotation and $R = 1$ is the liquid-air interface which is assumed to be planar.

The Reynolds Number, R_e , represents the measure of inertial stresses relative to viscous stresses. Viscometers are usually analyzed by considering the "inertialless" limit of $R_e \rightarrow 0$, in which case the flow consists of circular streamlines. Viscometers generally operate with a gap-to-radius ratio, λ , of less than 0.05 and with the product λR_e less than unity.

III. NUMERICAL PROCEDURE

To solve the Navier-Stokes equations, Chorin's explicit technique is used. An artificial compressibility factor, δ , is introduced into the equations of motion. Hence the continuity equation is replaced by

$$\frac{\partial D}{\partial T} = -\lambda \left(\frac{U}{R} + \frac{\partial U}{\partial R} \right) - \frac{\partial W}{\partial Z} \quad (9)$$

where $P = D/\delta$ is an artificial equation of state.

Equations (5), (6), (7), and (9) are put into finite difference form by means of a Dufort-Frankel scheme, (details are obtained from Chorin [1]), and the resultant equations appearing below are then utilized in the computing procedure:

$$U(T^+) = \left\{ -\frac{\lambda \Delta T}{\Delta R} U [U(R^+) - U(R^-)] \right.$$

$$+ 2\lambda \Delta T \frac{V^2}{R}$$

$$- \frac{\Delta T}{\Delta Z} W [U(Z^+) - U(Z^-)]$$

$$- \frac{\lambda \Delta T}{\delta \Delta R} [D(R^+) - D(R^-)]$$

$$+ \frac{2\lambda^2 \Delta T}{R_e \Delta R^2} [U(R^+) + U(R^-) - U(T^-)]$$

$$+ \frac{\lambda^2 \Delta T}{R_e \Delta R} \frac{[U(R^+) - U(R^-)]}{R}$$

$$- \frac{2\lambda^2 \Delta T}{R_e} \frac{U}{R^2}$$

$$+ \frac{2\Delta T}{R_e \Delta Z^2} [U(Z^+) + U(Z^-) - U(T^-)]$$

$$+ U(T^-) \} / \left\{ 1 + \frac{2\lambda^2 \Delta T}{R_e \Delta R^2} + \frac{2\Delta T}{R_e \Delta Z^2} \right\} \quad (10)$$

$$\begin{aligned}
V(T^+) = & \left\{ -\frac{\lambda \Delta T}{\Delta R} U [V(R^+) - V(R^-)] \right. \\
& - 2\lambda \Delta T \frac{UV}{R} \\
& - \frac{\Delta T}{\Delta Z} W [V(Z^+) - V(Z^-)] \\
& + \frac{2\lambda^2 \Delta T}{R_e \Delta R^2} [V(R^+) + V(R^-) - V(T^-)] \\
& + \frac{\lambda^2 \Delta T}{R_e \Delta R} \left[\frac{V(R^+) - V(R^-)}{R} \right] \\
& - \frac{2\lambda^2 \Delta T}{R_e} \frac{V}{R^2} \\
& + \frac{2\Delta T}{R_e \Delta Z^2} [V(Z^+) + V(Z^-) - V(T^-)] \\
& \left. + V(T^-) \right\} / \left\{ 1 + \frac{2\lambda^2 \Delta T}{R_e \Delta R^2} + \frac{2\Delta T}{R_e \Delta Z^2} \right\} \quad (11)
\end{aligned}$$

$$W(T^+) = \left\{ -\frac{\lambda \Delta T}{\Delta R} U [W(R^+) - W(R^-)] \right.$$

$$- \frac{\Delta T}{\Delta Z} W [W(Z^+) - W(Z^-)]$$

$$- \frac{\Delta T}{\delta \Delta Z} [D(Z^+) - D(Z^-)]$$

$$+ \frac{2\lambda^2 \Delta T}{R_e \Delta R^2} [W(R^+) + W(R^-) - W(T^-)]$$

$$+ \frac{\lambda^2 \Delta T}{R_e \Delta R} \left[\frac{W(R^+) - W(R^-)}{R} \right]$$

$$+ \frac{2\Delta T}{R_e \Delta Z^2} [W(Z^+) + W(Z^-) - W(T^-)]$$

$$+ W(T^-) \left. \right\} / \left\{ 1 + \frac{2\lambda^2 \Delta T}{R_e \Delta R^2} + \frac{2\Delta T}{R_e \Delta Z^2} \right\} \quad (12)$$

$$D(T^+) = -2\lambda\Delta T \frac{U}{R}$$

$$- \frac{\lambda\Delta T}{\Delta R} [U(R^+) - U(R^-)]$$

$$- \frac{\Delta T}{\Delta Z} [W(Z^+) - W(Z^-)] + D(T^-) \quad (13)$$

where $U(R^+) = U(R + \Delta R, Z, T)$;

$U(R^-) = U(R - \Delta R, Z, T)$; etc.

Equations (10) through (13) are applicable only at interior points. For the various boundaries, the following equations were developed using for the purpose one-sided differences.

At the centerline, ($R = 0$),

$$U = 0 \quad (14)$$

$$V = 0 \quad (15)$$

$$W(T^+) = \left\{ - \frac{\Delta T}{\Delta Z} W [W(Z^+) - W(Z^-)] \right.$$

$$\left. - \frac{\Delta T}{\delta\Delta Z} [D(Z^+) - D(Z^-)] \right.$$

$$\left. + \frac{2\lambda^2\Delta T}{R_e\Delta R^2} [2W(R^+) - W(T^-)] \right\}$$

$$\begin{aligned}
 & + \frac{2\Delta T}{R_e \Delta Z^2} [W(Z^+) + W(Z^-) - W(T^-)] \\
 & + W(T^-) \} / \left\{ 1 + \frac{2\lambda^2 \Delta T}{R_e \Delta R^2} + \frac{2\Delta T}{R_e \Delta Z^2} \right\} \quad (16)
 \end{aligned}$$

$$\begin{aligned}
 D(T^+) = & - \frac{2\lambda \Delta T}{\Delta R} U(R^+) \\
 & - \frac{\Delta T}{\Delta Z} [W(Z^+) - W(Z^-)] + D(T^-). \quad (17)
 \end{aligned}$$

At the liquid-air interface, ($R = 1$),

$$U = 0 \quad (18)$$

$$\begin{aligned}
 V(T^+) = & \left\{ - \frac{\Delta T}{\Delta Z} W [V(Z^+) - V(Z^-)] \right. \\
 & + \frac{\lambda^2 \Delta T}{R_e \Delta R^2} [2V(R^-) - 4(R^-) + V(T^-)] \\
 & + \frac{2\Delta T}{R_e \Delta Z^2} [V(Z^+) + V(Z^-) - V(T^-)] \\
 & \left. + V(T^-) \right\} / \left\{ 1 - \frac{\lambda^2 \Delta T}{R_e \Delta R^2} + \frac{2\Delta T}{R_e \Delta Z^2} \right\} \quad (19)
 \end{aligned}$$

$$\begin{aligned}
W(T^+) = & \left\{ -\frac{\Delta T}{\Delta Z} W [W(Z^+) + W(Z^-)] \right. \\
& - \frac{\Delta T}{\delta \Delta Z} [D(Z^+) - D(Z^-)] \\
& + \frac{\lambda^2 \Delta T}{R_e \Delta R^2} [2W(R^{--}) - 4W(R^-) + W(T^-)] \\
& + \frac{2\Delta T}{R_e \Delta Z^2} [W(Z^+) + W(Z^-) - W(T^-)] \\
& \left. + W(T^-) \right\} / \left\{ 1 - \frac{\lambda^2 \Delta T}{R_e \Delta R^2} + \frac{2\Delta T}{R_e \Delta Z^2} \right\} \quad (20)
\end{aligned}$$

$$\begin{aligned}
D(T^+) = & \frac{2\lambda \Delta T}{\Delta R} U(R^-) \\
& - \frac{\Delta T}{\Delta Z} [W(Z^+) - W(Z^-)] + D(T^-). \quad (21)
\end{aligned}$$

Along the rotating disk, ($Z = 0$),

$$U = 0 \quad (22)$$

$$V = R \quad (23)$$

$$W = 0 \quad (24)$$

$$D(T^+) = -2 \frac{\Delta T}{\Delta Z} [W(Z^+) - W(Z^-)] + D(T^-) \quad (25)$$

Along the stationary disk ($Z = 1$),

$$U = 0 \quad (26)$$

$$V = 0 \quad (27)$$

$$W = 0 \quad (28)$$

$$D(T^+) = -2 \frac{\Delta T}{\Delta Z} [W(Z) - W(Z^-)] + D(T^-) \quad (29)$$

The above equations (to obtain steady state solutions) were programmed for a digital computer. Such solutions are considered to have been achieved when $D(T^+)$ and $D(T^-)$ are approximately equal. A copy of the computer program, coded in Fortran IV, is contained in Appendix A.

IV. STABILITY

If the flow under consideration is to remain incompressible and therefore stable, Chorin asserts that δ must be chosen so that

$$\delta^{\frac{1}{2}} R_e \text{ Max}_{R, Z} (U^2 + V^2 + W^2)^{\frac{1}{2}} < 1.$$

This is equivalent to keeping the artificial Mach Number less than unity.

To insure that motion can be adequately described in the confines of a given grid scheme ΔT must be chosen so that

$$\Delta T \leq .437 \text{ Min}_{R, Z} (\Delta R \text{ or } \Delta Z) \delta^{\frac{1}{2}}.$$

Numerical results show that the above conditions are not sufficient for stability in some cases and too restrictive in others.

V. NUMERICAL RESULTS AND DISCUSSION

The secondary flows found in the R-Z plane are shown for $\lambda = 1.0, .50, .20$ and $.10$ in Figures 3 through 6. ($\lambda R_e = 1.0$ in each case.) Computer program outputs for velocities and pressures corresponding to these cases are given in Appendix B.

Once an adequate δ and ΔT are chosen, convergence is achieved in 2000 to 4000 iterations. This requires 20 to 40 minutes of computer time. The following table contains δ and ΔT values for which divergence occurs:

λ	R_e	Trial Values		Chorin's Necessary Conditions	
		δ	ΔT	δ	ΔT
.75	1.0	.04	.001	1.0	.022
.75	1.0	.09	.001	1.0	.022
.75	1.0	.16	.001	1.0	.022
1.0	1.0	.04	.0005	1.0	.022

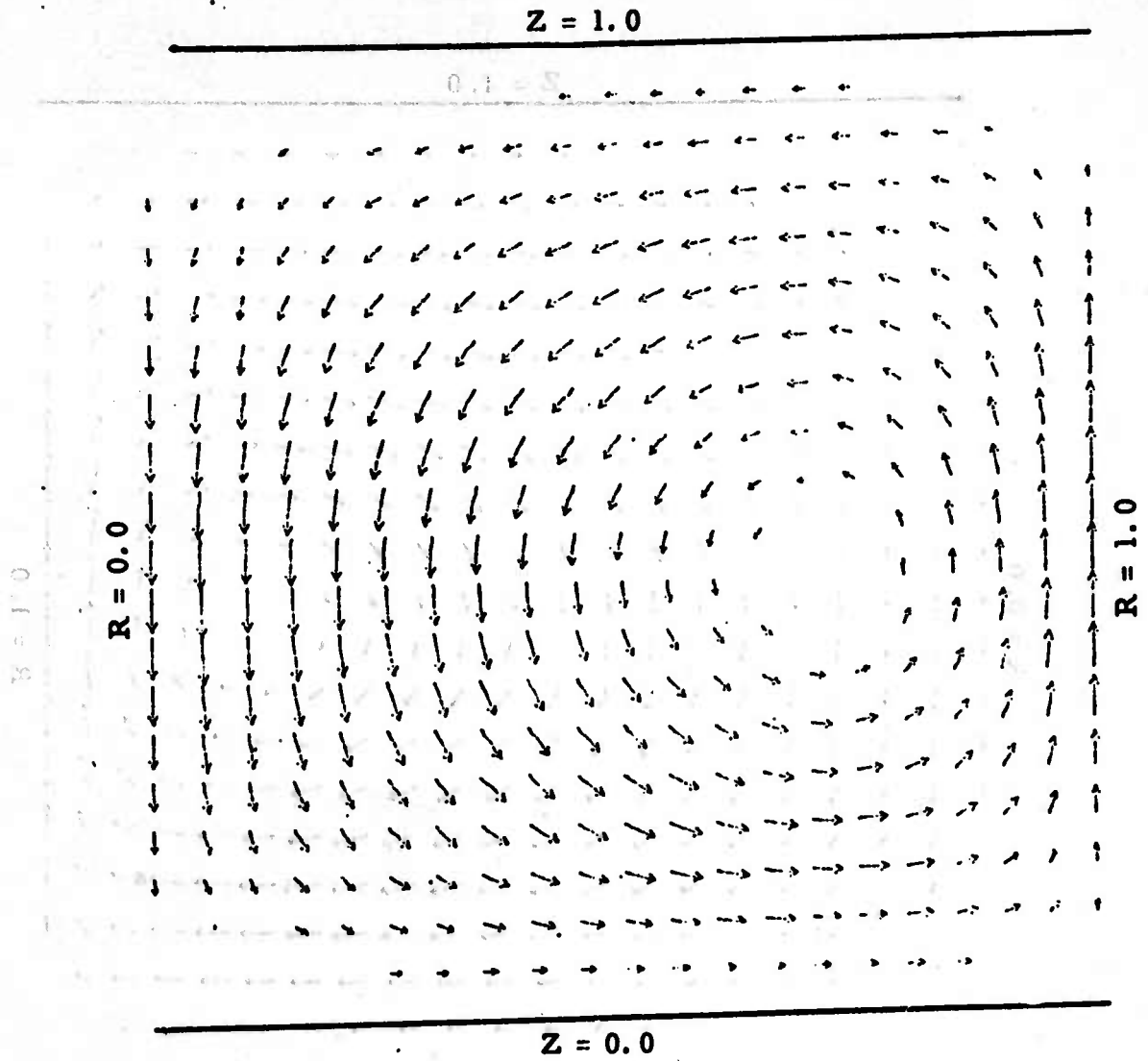


Figure 3. Secondary Velocity Field

($\lambda = 1.0, R_e = 1.0$)

Scale: $.25'' = .00458$

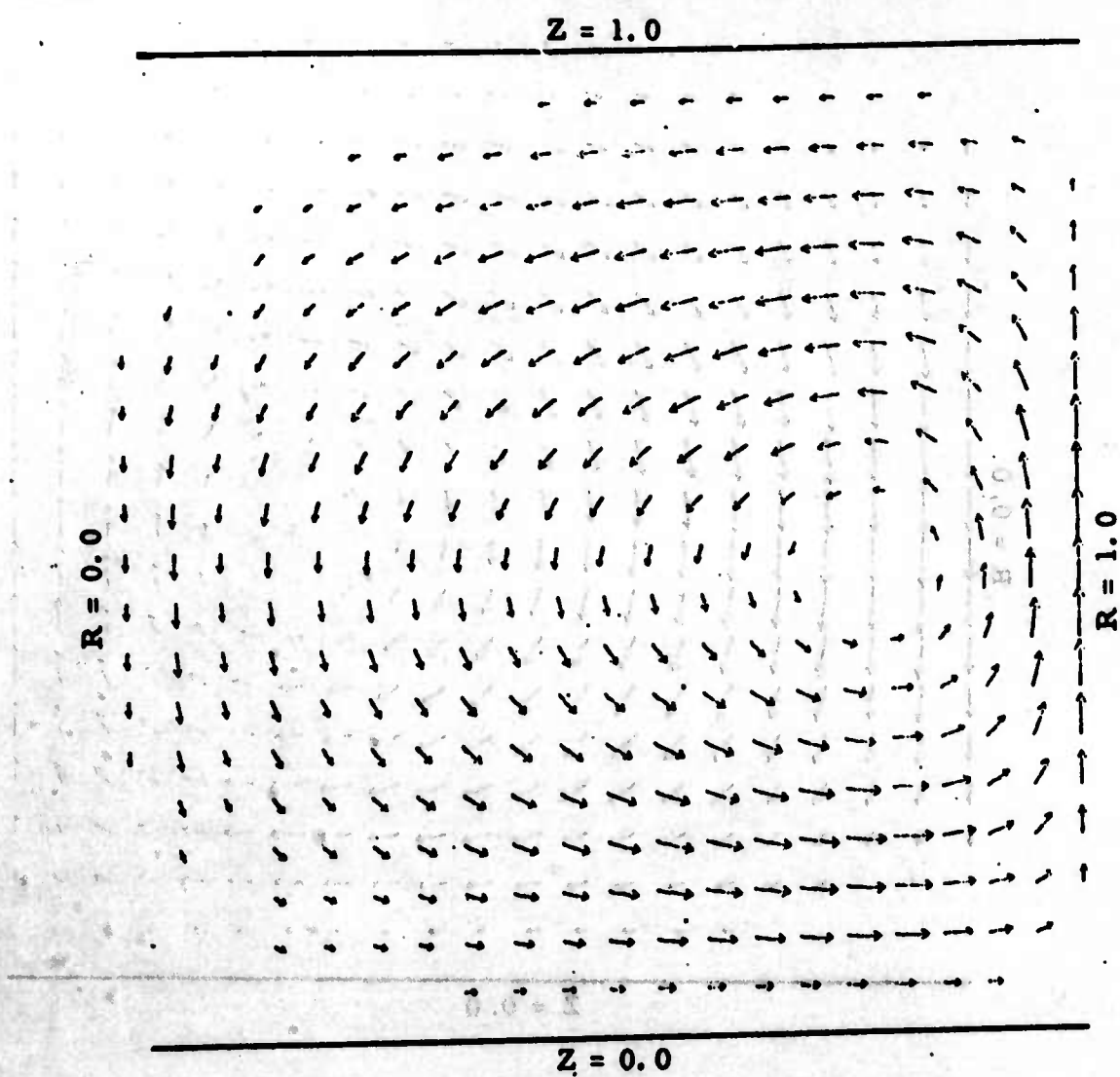


Figure 3. Secondary Velocity Field

(Figure 4. Secondary Velocity Field)

($\lambda = .5, R_e = 2.0$)

Scale: $.25'' = .00636$

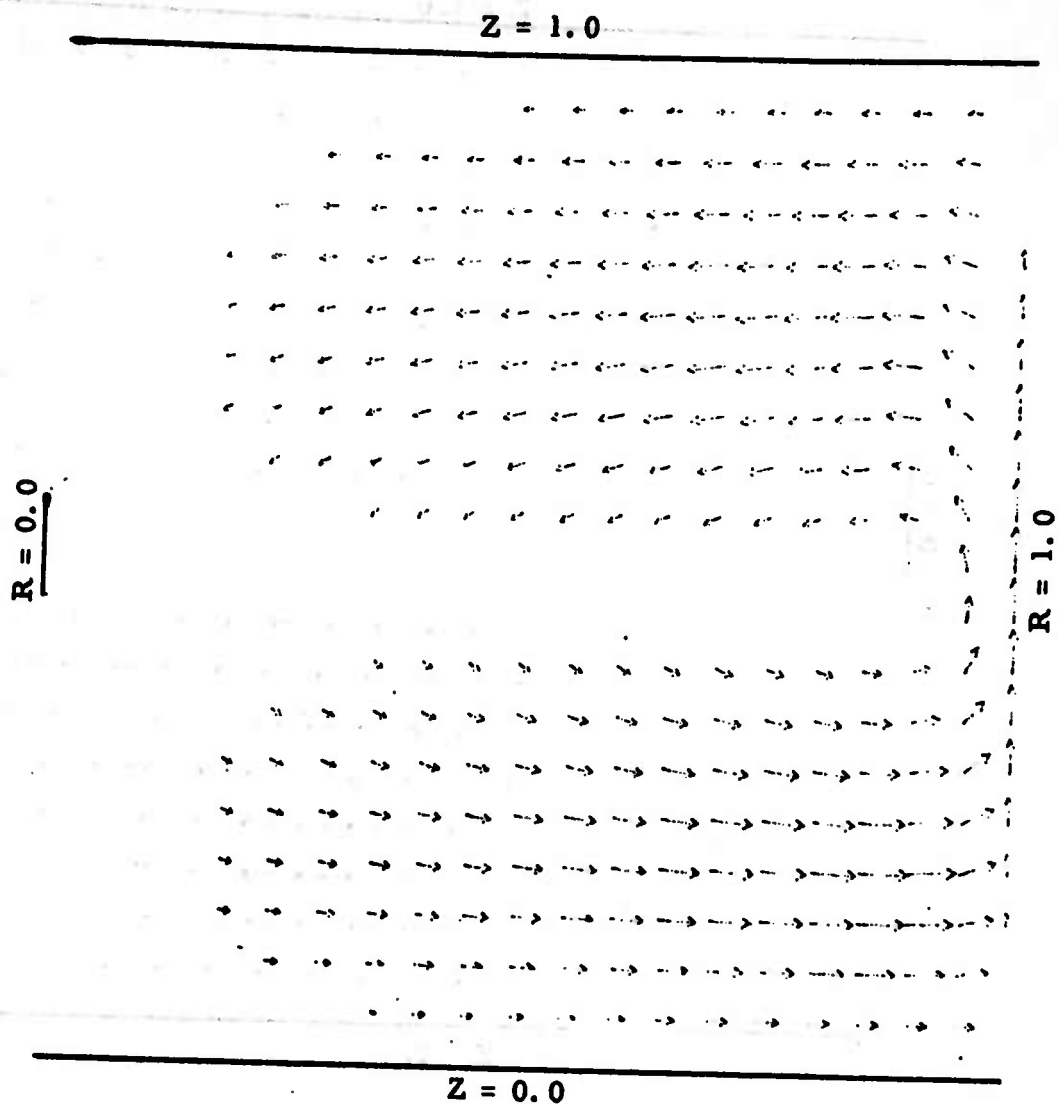


Figure 5. Secondary Velocity Field

($\lambda = .2$, $R_e = 5.0$)

Scale: $.25'' = .00677$

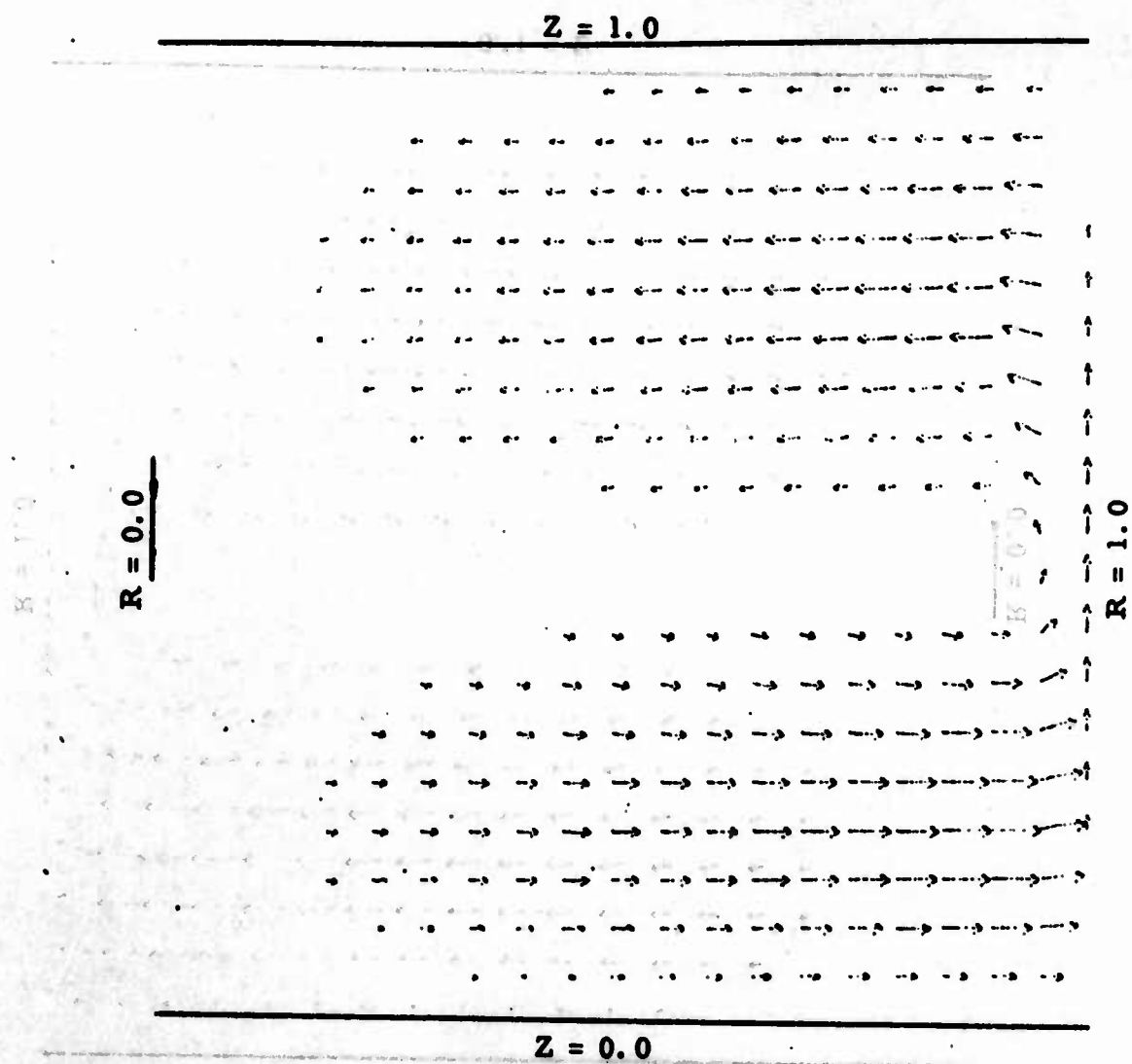


Figure 6. Secondary Velocity Field
 ($\lambda = .1, R_e = 10.0$)
 Scale: $.25'' = .00740$

Listed below are δ and ΔT values for which there are convergent solutions:

δ	R_e	Trial Values		Chorin's Necessary Conditions	
		δ	ΔT	δ	ΔT
1.0	1.0	.04	.00025	1.0	.022
.75	1.0	.04	.00075	1.0	.022
.75	1.0	.04	.00075	1.0	.022
.75	1.0	.09	.00075	1.0	.022
.75	1.0	.16	.0005	1.0	.022
.75	1.0	.16	.00075	1.0	.022
.75	10.0	.04	.0005	.01	.002*
.50	1.0	.09	.001	1.0	.022
.50	2.0	.04	.001	.25	.011
.20	1.0	.09	.001	1.0	.022
.20	5.0	.04	.0005	.04	.004
.20	5.0	.04	.001	.04	.004
.10	1.0	.04	.001	1.0	.022
.10	10.0	.04	.001	.01	.002*
.10	5.0	.04	.001	.04	.004

*The necessary conditions are violated, yet a convergent solution is obtained.

At least 20 grid spaces are necessary in R and Z for reasonable results. Numerical oscillations are produced in the Z direction when only ten grid spaces are used.

For the small secondary flows, true convergence is very difficult to discern with this numerical technique. As an example, for $\lambda = .1$ and $R_e = 5.0$ convergence seems to have been achieved in 2000 iterations. But when the results are plotted, numerical oscillations in U are evident. However, after 4000 iterations these oscillations have vanished and the results appear to be accurate when compared with the infinite disk solution.

Rate of convergence is independent of starting values unless accurate values at $R = 1.0$ for W are introduced. In proof of this, a case was run which took as an initial state the infinite disk solution. Convergence still required 2000 iterations.

In order to test the stability of the numerical solution, two special computer runs were made. In the first, a convergent solution was perturbed in W. This perturbation was of the order $\text{Max}|W|$ and R, Z was introduced between $R = 0.5$ and 0.6 . The solution again converged, suggesting stability for finite perturbations. For the second run, initial values were assumed from the infinite disk solution and pressure was increased by an order of magnitude. This solution achieved an oscillatory behavior then diverged completely.

VI. CONCLUSIONS

A large scale parametric examination of δ , ΔT , ΔR and ΔZ is required to best determine the numerical stability, the rate of convergence, and the accuracy of each problem solved using Chorin's technique. To show that the results obtained herein are indeed reasonable a numerical solution is compared with a series solution for infinite disks. The series solutions are written to second order in λR_e as follows [2, 3]:

$$\dot{U} = - \frac{\lambda R_e}{60} [4 (1-Z) - 9 (1-Z)^2 + 5 (1-Z)^4]$$

$$V = R (1-Z) - \frac{\lambda^2 R_e^2}{6300} [- 8 (1-Z) - 35 (1-Z)^4 + 63 (1-Z)^5 - 20 (1-Z)^7]$$

$$W = \frac{\lambda R_e}{60} [- 4 (1-Z)^2 + 6 (1-Z)^3 - 2 (1-Z)^5]$$

$$P = .15 R^2 .$$

These comparisons are made for $\lambda = .1$ and $R = 5.0$. Figure 7 shows the secondary velocity field for the numerical solution. (A computer output for this solution is contained in Appendix B.)

Z = 1.0

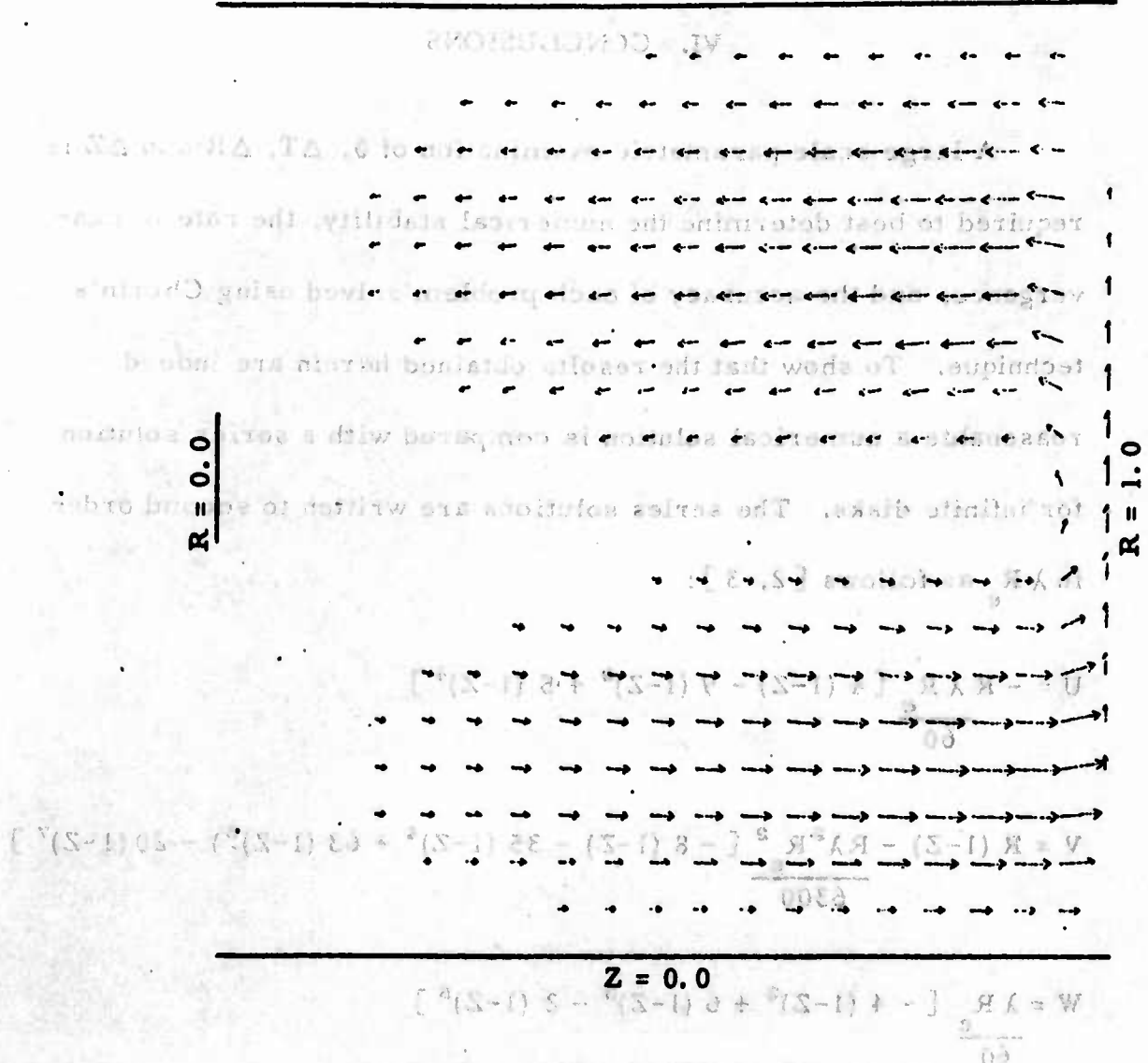


Figure 7. Secondary Velocity Field

($\lambda = .1, R_e = 5.$)

Scale: .25" = .00369

These comparisons are made for $\lambda = .1$ and $R = 5.0$. Figure 7 shows

the secondary velocity field for the numerical solution. (A comparison

output for this solution is contained in Appendix B.)

Figure 8 shows a graphical representation of a comparison between the numerical solution for finite disks and the series solution for infinite disks.

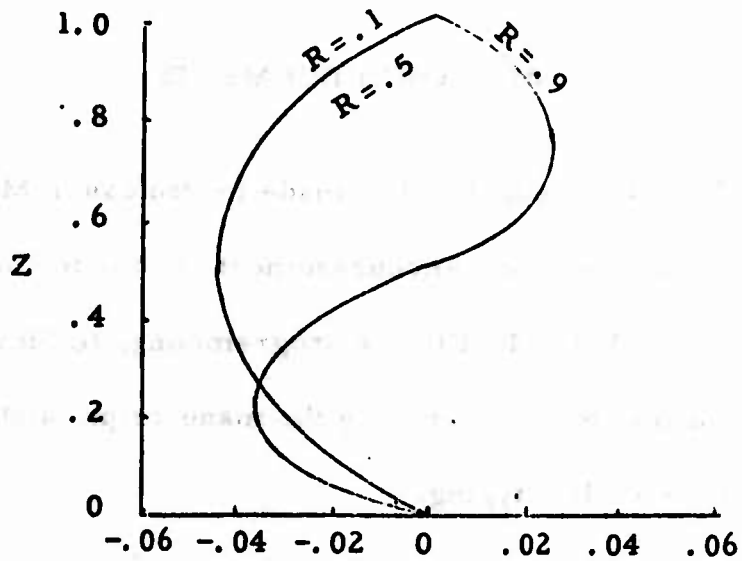


Figure 8. $\frac{U - U_{\infty}}{R \text{ Max } U_{\infty}}$
R, Z

Considering the closeness of the results of the above comparison it can definitely be stated that the velocity and pressure for rotating disk viscometer applications are adequately represented by the series solution of the infinite disk problem.

ACKNOWLEDGEMENTS

Grateful acknowledgement is made to Professor Morton M. Denn for his assistance and encouragement, to Monte Coleman for assistance with CALCOMP Plotter programming, to Muriel Ewing for helpful suggestions in preparing the manuscript, and to Alcise Beatty for the excellent typing.

VII. REFERENCES

1. Chorin, Alexandre Joel, "A Numerical Method for Solving Incompressible Viscous Flow Problems," *Journal of Computational Physics*, Vol. 2, No. 1, Aug. 1967, pp. 12-26.
2. Mellor, G. L.; Chapple, P. J.; and Stokes, V. K., "On Flow Between a Rotating and a Stationary Disk," *Journal of Fluid Mechanics*, Vol. 31, Part 1, 1968, pp. 95-112.
3. Catania, Peter, Through personal contact, 1970.
4. Whitaker, Stephen, "Introduction to Fluid Mechanics," 1st ed., Englewood Cliffs, New Jersey, Prentice-Hall, Inc., p. 155.

APPENDIX A

COMPUTER PROGRAM

Coding hints:

1. Factor all constants and remove their computation from the innermost integration loop. This results in a 30% reduction of computer time.

2. Simplify the subscript arithmetic as much as possible. (See statement number 5.) This results in a 20% reduction of computer time.

```

DIMENSION U(51,21,3),V(51,21,3),H(51,21,3),O(51,21,3),R(51),Z(21)
REAL LAM
READ(5,51)LAM,RE,DEL,DT,DR,DZ,L,M
N=1
R(1)=0.
Z(1)=0.
LMI=L-1
MMI=M-1
DO 2 I=1,LMI
R(I+1)=R(I)+DR
DO 20 I=1,MMI
Z(I+1)=Z(I)+DZ
DO 3 I=1,LMI
DO 3 J=1,MMI
DO 3 K=1,3
U(I,J,K)=0.0
V(I,J,K)=0.0
W(I,J,K)=0.0
D(I,J,K)=0.0
DO 4 I=1,LMI
DO 4 K=1,3
V(I,1,K)=R(I)
WRITE(6,52) RE,DT,DR
LAM2=LAM**2
DR2=DR**2
CZ2=DZ**2
DIV1=1.0+DT*(-LAM2/DR2+2.0/DZ2)/RE
DIV=1.0+2.0*DT*(LAM2/DR2+1.0/DZ2)/RE
RDIV=1.0/DIV

```

1

2

20

3

4

```

RDIV1=1.0/DIV1
C1=LAM*DT/DR
C2=2.0*LAM*DT
C3=DT/DZ*(0.01*(VMS1003+P.0/DIS)/6E
C4=LAM*DT/(DR*DEL)*(DRS+5.0/DS)*KE
C5=2.0*LAM2*DT/(RE*DR2)
C6=LAM2*DT/(RE*DR)
C7=2.0*LAM2*DT/RE
C8=2.0*DT/(RE*DZ2)
C9=DT/(DEL*DR)
C10=LAM2*DT/(RE*DR2)
C11=DT/(DEL*DZ)
C12=2.0*DT/DZ
C13=2.0*LAM*DT/DR
S DO 6 J=2,MH1
(NJ=(J-1)*51)
(NJP=J*51)
(NJN=(J-2)*51)
DO 6 I=2,LM1
(IJ=NJ+I(1)+DI)
(IJP=NJP+I*MH)
(IJN=NJN+I*DB)
(U(IJ,1,3))=(-U(IJ,1,2)+(U(IJ+1,1,2)-U(IJ-1,1,2))*C1)
(U(IJ,1,2))=(U(IJP,1,2)-U(IJN,1,2))*C3
(U(IJ,1,1,2))=D(IJ-1,1,2))*C4
(U(IJ,1,1,2))+U(IJ-1,1,2)-U(IJ,1,1))*C5
(U(IJ,1,1,2))-U(IJ-1,1,2))/R(I)
(U(IJP,1,2))/R(I)*2*(DR*DS)*FOM
(U(IJ,1,2))+U(IJN,1,2)-U(IJ,1,1))*C8

```

DIRECTION U(21,1,3)+A(21,1,3)*M(21,1,3)+I(21,1,3)+R(21,1,3)

```

S+U(IJ,1,1))*RDIV
V(IJ,1,3)=-U(IJ,1,2)*(V(IJ+1,1,2)-V(IJ-1,1,2))*C1
S-C2*U(IJ,1,2)+V(IJ,1,2)/R(I)
S-W(IJ,1,2)*(V(IJP,1,2)-V(IJN,1,2))*C3
S+(V(IJ+1,1,2)+V(IJ-1,1,2)-V(IJ,1,1))*C5
S+C6*(V(IJ+1,1,2)-V(IJ-1,1,2))/R(I)
S-C7*V(IJ,1,2)/R(I)*2
S+(V(IJP,1,2)+V(IJN,1,2)-V(IJ,1,1))*C8
S+V(IJ,1,1))*RDIV
W(IJ,1,3)=-U(IJ,1,2)*(W(IJ+1,1,2)-W(IJ-1,1,2))*C1
S-W(IJ,1,2)*(W(IJP,1,2)-W(IJN,1,2))*C3
S-(D(IJP,1,2)-D(IJN,1,2))*C9
S+(W(IJ+1,1,2)+W(IJ-1,1,2)-W(IJ,1,1))*C5
S+C6*(W(IJ+1,1,2)-W(IJ-1,1,2))/R(I)
S+(W(IJP,1,2)+W(IJN,1,2)-W(IJ,1,1))*C8
S+W(IJ,1,1))*RDIV
D(IJ,1,3)=-C2*U(IJ,1,2)/R(I)
S-(U(IJ+1,1,2)-U(IJ-1,1,2))*C1
S-(W(IJP,1,2)-W(IJN,1,2))*C3+D(IJ,1,1)
CONTINUE
DO 7 J=2,MM1
V(L,J,3)=(12.0*V(L-2,J,2)-4.0*V(L-1,J,2)+V(L,J,1))*C10
S-W(L,J,2)*(V(L,J+1,2)-V(L,J-1,2))*C3
S+(V(L,J+1,2)+V(L,J-1,2)-V(L,J,1))*C8
S+V(L,J,1))*RDIV1
W(1,J,3)=-W(1,J,2)*(W(1,J+1,2)-W(1,J-1,2))*C3
S-(D(1,J+1,2)-D(1,J-1,2))*C11
S+(2.0*W(2,J,2)-W(1,J,1))*C5
S+(W(1,J+1,2)+W(1,J-1,2)-W(1,J,1))*C8

```

6

C


```

10      W(I,J,1)=W(I,J,2)
        D(I,J,2)=D(I,J,3)
        D(I,J,1)=D(I,J,2)
        CONTINUE
        DMAX=0.0
        DO 100 I=1,L
        DO 100 J=1,M
        CMAX=AMAX1(DMAX,ABS(D(I,J,3)))
        IF(DMAX.GT.1.0)GO TO 101
        N=N+1
        IF(MOD(N,100).NE.0)GOTO 5
        WRITE(6,53)N
        WRITE(6,51)LAM,RE,DEL,DT,DR,DZ,L,M
        WRITE(6,54)
        LMT=LMI/10
        JMT=MMI/10
        J=M
11      WRITE(6,50)(U(I,J,3),I=1,L,LMT)
        J=J-JMT
        IF(J.GT.0)GOTO 11
        WRITE(6,52)
        WRITE(6,55)
        J=M
12      WRITE(6,50)(V(I,J,3),I=1,L,LMT)
        J=J-JMT
        WRITE(6,52)
        IF(J.GT.0)GOTO 12
        WRITE(6,56)
        J=M
13      WRITE(6,50)(W(I,J,3),I=1,L,LMT)

```



```

13 J=J-JMT
IF(J.GT.0)GOTO 13
WRITE(6,52)
WRITE(6,57)
J=M
14 WRITE(6,50)(D(1,J,3),I=1,L,LMT)
J=J-JMT
IF(J.GT.0)GOTO 14
IF(N.LT.4000.AND.DMAX.LT.1.0)GO TO 5
GOTO 1
STOP
50 FORMAT(1F7.5)
51 FORMAT(6F10.6,2I10)
52 FORMAT(//)
53 FORMAT(3HIN=,(5)
54 FORMAT(2H U)
55 FORMAT(2H V)
56 FORMAT(2H W)
57 FORMAT(2H O)
END
101 16(9*2)M
102 16(10M*100)VE*0100 2
H=M+1
103 16(DVX*01*1*0100 10 101
DVX=YVXVXNDVXVX*2(11*7*3))
00 100 1=1*
J=1 1
00 100 1=1*
DVX=0.0
104 CONTINUE
011*11=0111*151
011*11=0111*131
011*11=0111*131
011*11=0111*131

```

APPENDIX B

SAMPLE COMPUTER OUTPUTS

Guide to the computer output:

1. The first line of print is the number of iterations.
2. The second line of print is λ , R_e , δ , ΔT , ΔR , ΔZ and a pair of indices.
3. The velocity fields (U, V, W) and the density ($D = \delta P$) are printed on the following lines. The numbers are oriented so as to correspond to the graphs previously shown.

N= 4000	U	1.000000	1.000000	0.040000	0.000250	0.050000	0.050000	21	21
.00000	.00000	.00000	.00000	.00000	.00000	.00000	.00000	.00000	.00000
.00000	.00032	.00081	.00127	.00165	.00190	.00200	.00189	.00155	.00092
.00000	.00049	.00116	.00179	.00229	.00261	.00271	.00254	.00203	.00117
.00000	.00047	.00111	.00169	.00215	.00245	.00254	.00236	.00188	.00108
.00000	.00032	.00075	.00115	.00146	.00167	.00174	.00163	.00131	.00076
.00000	.00009	.00021	.00031	.00040	.00047	.00051	.00052	.00045	.00028
.00000	.00018	.00043	.00066	.00084	.00094	.00094	.00082	.00060	.00031
.00000	.00042	.00101	.00156	.00199	.00227	.00234	.00216	.00168	.00094
.00000	.00056	.00133	.00206	.00266	.00308	.00324	.00307	.00249	.00145
.00000	.00043	.00108	.00172	.00226	.00266	.00287	.00281	.00239	.00148
.00000	.00000	.00000	.00000	.00000	.00000	.00000	.00000	.00000	.00000
.00000	.00000	.00000	.00000	.00000	.00000	.00000	.00000	.00000	.00000
.00000	.01000	.02001	.03001	.04002	.05003	.06004	.07006	.08008	.09009
.00000	.02001	.04001	.06002	.08004	.10006	.12008	.14011	.16015	.18018
.00000	.03001	.06001	.09003	.12004	.15007	.18011	.21015	.24020	.27025
.00000	.04000	.08001	.12002	.16004	.20007	.24011	.28016	.32023	.36030
.00000	.04999	.09999	.15000	.20001	.25004	.30009	.35015	.40023	.45031
.00000	.05998	.11997	.17997	.23998	.30001	.36005	.42012	.48020	.54029
.00000	.06998	.13996	.20995	.27995	.34997	.42001	.49006	.56014	.63024
.00000	.07998	.15995	.23994	.31994	.39995	.47997	.56002	.64008	.72016
.00000	.08998	.17997	.26996	.35995	.44996	.53997	.62999	.72003	.81008
.00000	.10000	.20000	.30000	.40000	.50000	.60000	.70000	.80000	.90000

